

---

# TOWARD RELIABLE SIGNALS DECODING FOR ELECTROENCEPHALOGRAM: A BENCHMARK STUDY TO EEGNeX

---

A PREPRINT

Xia Chen <sup>\* a</sup>

Xiangbin Teng<sup>b</sup>

Han Chen<sup>c</sup>

Yafeng Pan<sup>c</sup>

Philipp Geyer<sup>d</sup>

November 10, 2022

## ABSTRACT

*Objective:* This study aims to establish an essential milestone by leveraging an exhaustive performance analysis of common Neural networks' (NNs) capability to decipher mental representations from electroencephalogram (EEG) signals recorded in representative classification tasks. *Methods:* In this study, 14 mechanism-wise different, typical NN types and their variants were first constructed to decode EEG signals to compare their information representation capability based on four brain-computer interfaces BCI paradigms. Based on throughout literature review and the result, we gradually develop improvements to propose a novel, pure convolutional NN architecture: EEGNeX. We tested EEGNeX with existing advanced approaches and Mother of All BCI Benchmarks (MOABB), a large-scale test benchmark containing experiments in 11 different EEG motor imagination (MI) datasets. *Results:* The result reveals vital insights regarding the reliable development of the network architecture in BCI signal feature extraction and representation learning. EEGNeX outperforms other current state-of-the-art methods. Modifications are proven beneficial in universal NN improvement with statistical significance over EEGNet and common approaches. Four pillars are summarized to design NNs for efficient design EEG signal decoding. *Significance:* The study lightens a pathway based on the analysis results to gradually develop general improvements for analogy investigations between the brain bioelectric signal generation process and NN architecture. A novel NN architecture: EEGNeX, is proposed. We open-sourced all models in an out-of-the-box status (<https://github.com/chenxiachan/EEGNeX>) to support further interdisciplinary studies.

## 1 Introduction

The Brain-Computer Interface (BCI) study aims to research communication pathways between machine and brain signals [Wolpaw et al., 2000]. From the perspective of information theory, today's machine learning models, especially Neural Networks (NNs) [Schmidhuber, 2015], are increasingly similar to the human brain in many tasks [Hasson et al., 2020]: a universal structure to process, store and communicate input/output data that carries information. In this context, recent research has incorporated NNs into the BCI domain for feature extraction. Among all neuroimaging methods, one of the most widely used in BCI is electroencephalography (EEG) [Niedermeyer and Da Silva, 2005] because of its non-invasive recording with low risk and cost. NNs are advanced in accepting and processing EEG signals without prior knowledge to aid in understanding the human brain.

---

<sup>a</sup>Leibniz University Hannover, Germany <xia.chen@iek.uni-hannover.de>

<sup>b</sup>Department of Education and Psychology, Freie Universität Berlin, 14195 Berlin, Germany

<sup>c</sup>Department of Psychology and Behavioral Sciences, Zhejiang University, China

<sup>d</sup>Leibniz University Hannover, Germany

Performance advantages in decoding EEG have been well proved in various NN variations with the strength of implicit feature extraction and end-to-end representation learning ability. The majority of NNs adopted in the EEG community are Recurrent Neural Networks (RNNs, primarily referring to Long Short-Term Memory, LSTM [Hochreiter and Schmidhuber, 1997]; and Gated Recurrent Unit, GRU [Chung et al., 2014]) [Ruffini et al., 2016, Craik et al., 2019a], Convolutional Neural Networks (Conv. or CNNs) [Alzubaidi et al., 2021, Altaheri et al., 2021], and domain integrated structures, such as EEGNet [Lawhern et al., 2018]. Despite the widespread research, we noticed a gap that exists in the community: Most studies focus primarily on enhancing classification accuracy on a particular dataset or a type of task by incorporating manual feature extraction via different domain knowledge preprocessing [Craik et al., 2019a], regularization [Deng et al., 2021], incorporate data with signal transformation techniques [Huang et al., 2020, Altaheri et al., 2021] with fine-tuned hyperparameter models, making understanding the generalization performance of representation learning abilities among different NNs difficult. Thus, it remains unclear how those previous approaches perform in the same context and can be used to guide further improvement. In other words, in this paper, we try to answer the following two questions:

- *How well do different types of neural network models extract features from raw EEG data?*
- *How to design an efficient neural network for representation learning in the BCI domain?*

To address these questions, we make contributions in this study in three-fold:

1. We exhaustively evaluated the performance of 14 different fundamental NNs' accuracies in four EEG-based BCI classification task datasets under different paradigms. The comparison result revealed EEG-based information representation efficacy of different NNs. Four pillars are summarized to design an efficient NN for EEG-based classification tasks.
2. Based on the result, we provide a trajectory from an advanced NN architecture, namely, EEGNet, to EEGNeX, a pure convolution-based architecture. EEGNeX presents a performance advance with other similar end-to-end NNs. Compared to typical algorithm pipelines evaluated in Mother of All BCI Benchmarks (MOABB) [Jayaram and Barachant, 2018], EEGNeX shows higher accuracy with statistical significance on 11 diverse EEG motor imagination (MI) datasets.
3. We open-source all models and EEGNeX to bring a testbed for research and aim to reduce the difficulties of NN implementation in the BCI domain.

The remainder of this paper is organized as follows: Target datasets, different neural networks, and accuracy benchmark results are described in 2, followed by an analysis with a proposal of structural innovation based on EEGNet (3). the accuracy novelty of EEGNeX is validated in 4 with the discussion of the future direction in 5. 6 concludes the study.

## 2 Materials and Methodologies

### 2.1 Related research

This subsection briefly reviews the two major NN adaptation types and their development in EEG-based BCI classification tasks, followed by a parallel analogy of the NN development in their original domain.

The first well-known NN adaptation in EEG classification was ConvNet [Cecotti and Graser, 2010]. ConvNet comprises two convolutional layers for extracting temporal and spatial features with dense layers applied on a P300 task. A similar CNN-based approach with max-pooling layers [Schirrmeister et al., 2017] is applied and shows a performance advantage when compared with a well-known, domain-knowledge-based algorithm - filterbank common spatial patterns (FBCSP) [Chin et al., 2009]. EEGNet is based on the previous methods and further uses a combination of depthwise convolution with separable convolution [Lawhern et al., 2018]. With dropout layer, batch normalization layers, kernel constraint, and max-pooling stride, EEGNet claimed to have fewer parameters and more robust cross-sections performance than ShallowConvNet (with two convolution layers) and DeepConvNet (with five convolution layers). Due to the robustness and advanced performance implementation of EEGNet, several extended variations that combine domain knowledge are proposed: EEG-inception [Riyad et al., 2020] extended EEGNet by applying multi-head convolutions as an inception block with different kernel sizes (receptive fields) and pointwise convolution; Applying different narrow filter banks to the original signal with integration, FBCNet presents a hybrid approach combined with bandpass filtering to improve

performance on MI tasks [Mane et al., 2021]. EEG-TCNet [Ingolfsson et al., 2020] proposed adding a temporal convolutional network (TCN) [Bai et al., 2018] to strengthen the temporal feature extraction ability. EEG-ITNet [Salami et al., 2022] combines the above-mentioned two advanced structures: inception block and TC block, and claimed accuracy advance.

For RNN-based models, less attention has been drawn to the research of EEG classification tasks [Craik et al., 2019a]. A two-layer LSTM implementation is used for emotion recognition and achieves a performance advantage compared to statistical-based feature selection methods with traditional machine learning classifiers [Alhagry et al., 2017]. Similar LSTM implementations with feature extractors in MI tasks reported better performance than conventional methods and other deep networks, including CNN [Wang et al., 2018]. The other RNN variant, GRU, combined with the attention mechanism [Vaswani et al., 2017], has been applied to the emotion classification task [Chen et al., 2019]. The result shows that the GRU model with attention performs better than CNN and LSTM. Subsequently, a structure that combines CNN and LSTM is proposed for the same task with faster training time, in which CNNs are used to handle the spatial information from the EEG while RNNs extract the temporal information [Wilaiprasitporn et al., 2019].

Originally, CNNs and RNNs were primarily developed as classical models for tasks such as speech recognition (Natural Language Processing, NLP, temporal) and computer vision (CV, spatial) domain, respectively. The first intersection between them appears when the attention-based RNN Transformer, namely, BERT [Devlin et al., 2018] is proposed in language translation and ViT [Dosovitskiy et al., 2020] in image recognition. Although ViT performs better than traditional CNN architectures, e.g., VGGNet [Simonyan and Zisserman, 2014], ResNet [He et al., 2016], and EfficientNet [Tan and Le, 2019], the discussion of the advantages of such hybrid NN architectures is still ongoing: ConvNeXt [Liu et al., 2022] fine-adjusted the ResNet architecture to further improve to reach the level of Transformers in terms of accuracy and scalability while maintaining the simplicity and efficiency of standard convolution networks. Since BCI aims to interpret implicit information from brain activities that require both temporal and spatial decoding, it is meaningful to investigate different NNs' information representation processes to learn from their development path and adapt to the BCI domain.

## 2.2 Candidate methods

We focus on implementing performance comparison among two main types of NN structures: CNNs and RNNs, with their variations and combinations. Four basic layer types and their variations in TensorFlow [Abadi et al., 2016] were chosen for investigation: 2D convolution layer (**Conv2D**), 1D convolution layer (**Conv1D**), **LSTM** layer, **GRU** layer, and a combined single layer - **ConvLSTM2D**.

Moreover, several trending CNN variations whose mechanisms might affect the representation learning ability of NNs are chosen, including:

- **Depthwise separable convolutions** [Chollet, 2017]: consist of first performing a depthwise spatial convolution (which acts on each input channel separately) followed by a pointwise convolution that mixes the resulting output channels.
- **Causal padding**: initially designed in WaveNet [van den Oord et al., 2016] for sequential sound generation, as an implementation option in the Conv1D layer. It pads the layer's input with zeros in the front so values of early time steps can be predicted.
- **Dilation**: add the convolution layer with spaces in-between to support the exponential expansion of the receptive field without loss of resolution or coverage. It aggregates multi-scale contextual information and is firstly proposed for image semantic segmentation [Yu and Koltun, 2015].

Following the throughout reviews of EEG-based BCI classification tasks [Craik et al., 2019a, Hosseini et al., 2020], we reproduced common networks and adopted well-proved regulation procedures in corresponding NNs:

- Using kernel regularizers in RNNs.
- Using a CNN layer and batch normalization [Ioffe and Szegedy, 2015] with an exponential linear unit (ELU) activation function [Shah et al., 2016] as a standard CNN component.
- Adding average/max pooling layers at the final layer of CNN to account for local translation invariance.

A reproduction of EEGNet is integrated into the benchmark. In this study, we chose EEGNet-8,2, because of its better performance than EEGNet-4,2 (8 and 4 stand for different filter numbers of the first convolution layer in EEGNet), based on results from the original paper [Lawhern et al., 2018]. In this study, in total 14 NNs are chosen as candidates for the benchmark. Detailed architectures of all NN candidates are available in Appendix.

### 2.3 Datasets

To conduct a comprehensive and in-depth investigation of EEG representation learning and feature extraction capabilities on different NNs, we tested on four diverse EEG datasets with the consideration of covering within/cross-subjects, different tasks, paradigms, trial lengths, data sizes, and channels number. We present datasets as follows, with detailed descriptions and preprocessing procedures:

#### Event-related potential (ERP) – MindBigData

A single subject, 10-class ERP dataset [Vivancos, 2020]. This open database contains four different devices, 1,207,293 brain signals of 2 seconds long each. The signal records the imagine of presented digit images after exposing a subject to the visual stimulus of the MNIST dataset (from 0 to 9, -1 represents noise), resulting in similar phase synchrony among multiple channels for all classes. In this study, Emotive EPOC device data were selected. The raw EEG signals were recorded at a sample rate of 128 Hz; there are around 6500 trials for each digit image, with each trial containing 256 timesteps for 14 channels. We conducted a simple and common data preprocessing strategy, including: Noise events removal (-1); A combination of Butterworth lowpass filter (with a cutoff frequency of 63Hz) and a notch filter at 50Hz is applied on all trials; The first 32 timesteps (250ms) for each trial are trimmed to avoid noises caused by sensor power on.

#### Motor Imagery (MI) - OpenMBI Data

A 2-class MI data from Korea University EEG dataset [Lee et al., 2019]. The dataset contains 2-class EEG data from 54 healthy subjects with MI of left/right-hand classes in a total of 100 trials for each session in the length of 4s [Lee et al., 2019]. The original data is recorded at 1000Hz using 62 electrodes. As suggested by the original work, we selected 20 channels (FC-5/3/1/2/4/6, C-5/3/1/z/2/4/6, and CP-5/3/1/z/2/4/6) for the classification task. The EEG data is filtered with a notch of 1-40Hz and down-sampled at 128Hz.

#### Sensory Motor Rhythm (SMR) - BCIC-IV-2A Data

A 4-class SMR data from BCI Competition IV Dataset 2A [Tangermann et al., 2012]. This dataset consists of 22 EEG channels and 3 EOG channels from 9 subjects with the task of 4-class motor imagery (left hand, right hand, feet, tongue) classification. The sampling rate is 250 Hz with 0.5-100Hz notch filtered. In our analysis, we used all EEG channel signals with the entire trial.

#### Feedback Error-Related Negativity (ERN) - BCI challenge Data

A 2-class ERP data from BCI Challenge hosted by Kaggle [Margaux et al., 2012]. Detecting the ERN feedback helps to improve the performance of the P300 speller in the application. The dataset is used in the “BCI Challenge” to determine whether the P300 feedback is correct (2-class classification task), hosted by Kaggle [Margaux et al., 2012], consists of 26 healthy participants in 56 passive Ag/AgCl EEG sensors. The data is originally recorded at 600Hz, we used a 1-40Hz notch filter with 128Hz down-sampling for analysis.

Particularly, two (SMR and ERN) out of four chosen datasets are the same as in the original study of EEGNet [Lawhern et al., 2018] for comparative evaluation. SMR dataset is also adopted in model performance evaluation on EEG-inception, EEG-TCNet and EEG-ITNet studies. A characteristic overview of all datasets is presented in Table 1. The evaluation was chosen to be within-subject, as that minimizes the effect of non-stationarity. It is worth mentioning that some dataset collections in MOABB own small sample sets of data within-session, which increases the training difficulties of NN algorithms. The accuracy metric scores in 5-fold cross-validation to validate the general feature extraction & representation performance.

### 2.4 Training strategy

All datasets are grouped according to events (records of all channels for one event) and tested with candidate models for ten rounds under the same train/validation/test ratio of 0.75/0.125/0.125 (training data size equivalent to a 4-fold

Paradigm	Dataset	Subjects	Trials	Classes	Channels	Class Imbalance?	Size
ERP	MNIST of BRAIN DIGITS (MBD)	1	224	10	14	No	(64302, 14, 224)
MI	OpenMBI Data (MBI)	54	200	2	20	No	(10800, 20, 512)
SMR	BCIC-IV-2A Data (SMR)	9	500	4	22	No	(2592, 22, 500)
ERN	Feedback Error-Related Negativity (ERN)	26	160	2	56	Yes, ~3.4:1	(5440, 56, 160)

Table 1: Description of experiment dataset collections. Class imbalance, if present, is given as odds, means different classes have uneven odds, which is given as the average class imbalance over all subjects.

Dataset	MBD		MBI		SMR		ERN	
Model Name	Accuracy	Deviation	Accuracy	Deviation	Accuracy	Deviation	Accuracy	Deviation
Single_LSTM	13.31	0.49	53.78	0.79	27.38	2.59	71.43	0.53
Single_GRU	14.49	0.49	53.80	1.81	27.25	2.66	71.01	0.42
Conv1D	15.45	0.42	68.22	0.72	30.80	2.23	71.03	0.85
Conv1D_Dilated	15.11	0.28	69.87	0.69	31.64	3.06	70.31	0.74
Conv1D_Causal	15.11	0.44	67.71	0.96	30.62	2.91	69.31	0.35
Conv1D_CausalDilated	15.44	0.29	67.91	0.68	30.49	1.64	69.47	0.57
Conv2D	15.20	0.38	67.09	0.40	32.99	1.75	69.65	0.12
Conv2D_Dilated	15.15	0.29	68.76	0.81	33.46	1.96	68.88	0.28
Conv2D_Separable	16.26	0.45	68.67	0.90	34.72	3.13	72.26	0.10
Conv2D_Depthwise	16.20	0.28	68.90	0.75	36.51	2.27	71.54	0.43
Single_ConvLSTM2D	15.38	0.36	60.41	0.73	26.36	2.15	69.06	0.08
Conv_LSTM	15.77	0.34	69.57	0.80	30.77	1.63	69.90	0.42
Conv_GRU	15.75	0.31	67.48	0.80	29.41	1.68	71.85	0.19
EEGNet-8,2	<b>16.69</b>	0.29	<b>70.81</b>	0.91	<b>56.79</b>	2.06	<b>72.13</b>	0.37
EEGNet-8,2*	16.53	0.31	70.19	0.98	57.14	1.99	71.45	0.34

Table 2: Performance result of exhaustive evaluation on four datasets across all candidate models. The average accuracy and deviation are calculated based on ten rounds of the train-validation process with random seeds in the data split. In addition, model parameter sizes are presented along to represent the network complexity and search space size. To validate our implemented EEGNet performance, the Tensorflow version of EEGNet (with mark \*, <https://github.com/vlawhern/arl-eegmodels>) is included

cross-validation test) with random split seeds each round. As the sign-to-noise ratio of EEG signals is relatively low, NNs must avoid memorizing the noise components from EEG signals to end up overfitting the dataset.

To ensure that different modeling structures present their own best performance, all candidate methods were run under the same two-stage scheme: 1. With the training set under the batch size of 128 for each epoch with a default learning rate (0.001), the trained model accuracy is monitored on the validation set. The learning rate is reduced by half when accuracy stops improving for five epochs. The training process stops when there is no improvement for 20 epochs in the validation set to prevent overfitting; 2. Evaluate model performance by running on the test set. This two-stage strategy is designed to avoid data leakage and represent the performance of all benchmark models in the real-world production environment.

## 2.5 Experiment result

Table 2 presents the performance result of exhaustive evaluation on four datasets across all candidate models.

Based on the accuracy result among four datasets, some primitive findings regarding different NN architectures' performance are collected and categorized in three aspects:

- We noticed that those NNs designed to directly process sequences (RNNs and Conv1D with causal structure) are not ideal for direct EEG feature extraction and representation. Between LSTM and GRU models, we did not observe significant performance differences. Compared with RNNs, CNN-based models on average have higher classification accuracy. Given that all EEG datasets are multi-channel, **cross-channel spatial feature extraction is more efficient than direct compressed temporal information learning**.
- In the basic structure of CNNs, Conv2D generally achieved higher accuracy than Conv1D since it doesn't need to compress multi-channel EEG signals into a sequential format and learns patterns across channels. Among

different variations, separable 2D convolution architecture owns the best EEG feature extraction ability for learning temporal summary (Lawhern et al., 2018). The accuracy stability enhances with the combination of depthwise-separable 2D convolution and EEGNet. The key factor is that **the mechanism of depthwise convolution supports efficient cross-channel spatial feature learning**.

- The performance of hybrid model structures (CNN-LSTM, CNN-GRU) owns a considerable accuracy improvement over any single origin model. Particularly, we noticed that results of single layer ConvLSTM2D in all datasets are less accurate than Conv\_LSTM which consists of three stacked layers of Conv1D (see Appendix). It means that the single layer of NN is not sufficient for extracting information from EEG signals, combined with the fact of hybrid-models performance advance, which means **the additional temporal feature extraction after proper spatial filter/learning is beneficial for further model performance improvement**.

Based on the findings from the experiment result and literature review, we summarized four pillars that are considered contributitional to NN architecture design for efficient EEG-based BCI classification tasks: spatial filter, spatial (cross-channel) feature learning ability, temporal feature learning ability, and model parameter space and performance stability. We found that similar existing NN models are all benefited in performance improvement by strengthening at least one pillars. Figure 1 presents these key pillars and corresponding NN designs.

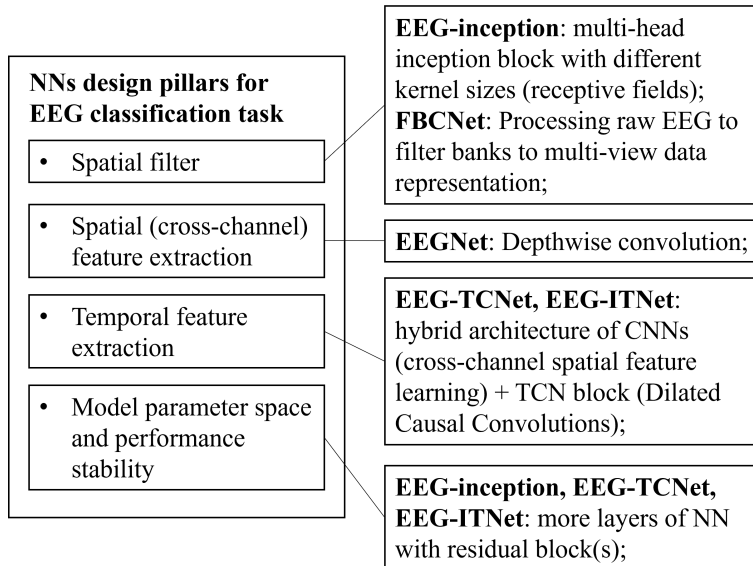


Figure 1: Network architecture design pillars for efficient EEG-based BCI classification tasks with proven models.

### 3 Roadmap: from EEGNet to EEGNeX

In the previous experiment, EEGNet presents the best performance among all candidate models, as: 1. The first part – the 2D convolution layer extracts the spectral representation of EEG input; 2. The second part – the kernel size of depthwise 2D convolution is tailored to the number of channels and directed to perform convolutions across channels. 3. The third part – separable 2D convolution conducted as feature extraction & learning. By revisiting the three parts mentioned above and adapting to modern network component designs, we can modify the EEGNet toward higher general performance.

In this section, we provide a trajectory going from an EEGNet to an EEGNeX that adopts findings from the last section, as well as some key component implementations of ConvNeXt [Liu et al., 2022]. The roadmap starts from a standard EEGNet with the adjustment of network architecture in different parts. Sequentially, component changes at the micro level are tested in the fixed network structure. We set the EEGNet as the backbone and tracked the successful steps tested on datasets described in Section 2 with proven performance improvement by ten rounds of validation. The summarized roadmap is as follows 4-steps: 1) Reinforce the spatial representation extraction from EEG input, 2) Replace the separable convolution with two 2D convolutions in the general architecture, 3) Inverse bottleneck structure,

4) Increase the receptive field of the layers with dilation and fewer activations. The modification purposes and detailed procedure with the results of each step are described as follows, and the quantitative result is presented in Figure 2.

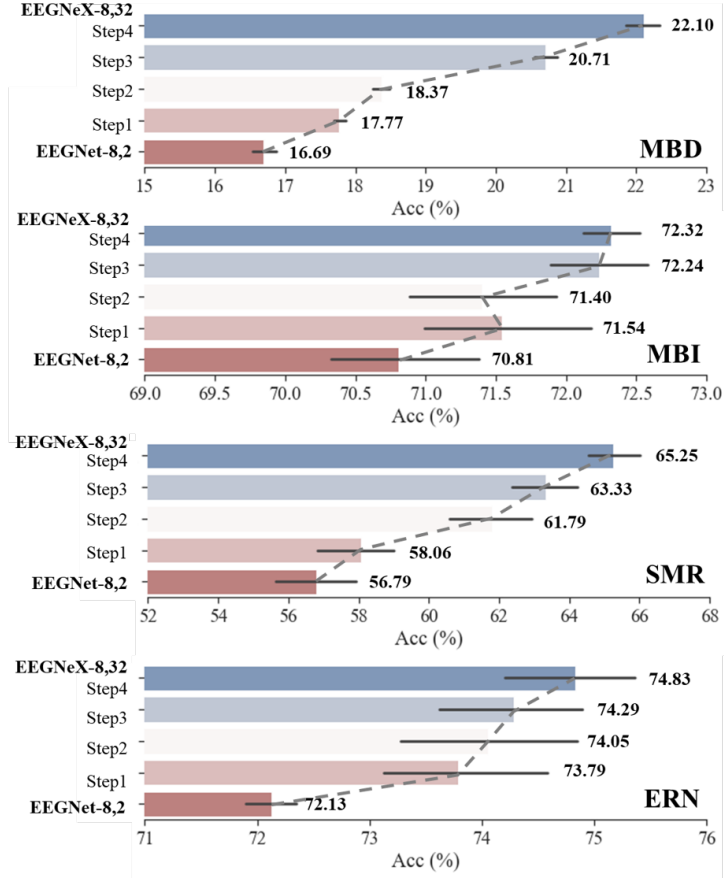


Figure 2: The roadmap of modifying from EEGNet - 8,2 toward EEGNeX - 8,32. The bars record the ten times average performance of the model at each step. The black horizontal lines represent the deviation to reflect model performance stability. In the end, the pure convolution-based network structure, namely EEGNeX, outperforms the EEGNet – 8,2 on all datasets.

### Step 1. Thicken the first part of spatial information extraction

Based on the study from Section 2, we noticed that the current structure of EEGNet is designed in three parts with the particular purpose of information processing. The first part that aims to extract spectral information from EEG input is shallow, with only one Conv2D block with a kernel size of 32 and output filters of 8. From the previous study [Schirrmeister et al., 2017] and considering the general network layer depth should not be too deep, we duplicate one more Conv2D block in the first part. It is worth mentioning that the adjustment we offered is the most intuitive solution. The key idea is to strengthen the network spatial feature extraction ability, and a more optimal design in this part is likely to exist (see Figure 1).

### Step 2. Replace the separable convolution with two 2D convolutions

This step focuses on understanding the second part of EEGNet, which is composed of a depthwise and a separable convolution. Depthwise convolutions are first proposed to use parameters more efficiently in the network trained with a large image dataset [Howard et al., 2017]. The advantage is two-fold: 1. The built-in mechanism acts as a cross-channel, frequency spatial learner (see Figure 3, subfigure c), which improves the global feature extraction abilities, especially adopted in multi-channel EEG. 2. It reduces network parameters and complexity; however, the EEG decoding domain normally deals with a dataset by using a shallower network structure compared to typical CNNs in the CV domain (ResNet, EfficientNet), making the improvement direction should aim to enhance the network parameter space.

Separable convolution is a method to factorize a convolution kernel into two smaller kernels [Howard et al., 2017] and consists of a depthwise convolution (cross-channels) and a pointwise convolution (1\*1 convolution to combine the outputs of the depthwise convolution). Since the channel dimension is compressed to one from the previous process, it makes separable convolution redundant. Combined with the direction of enhancing network parameter space, we drop the separable convolution and add an extra Conv2D block with a kernel size of 16 and output filters as 16 (8 → 16: depthwise convolutions with a depth multiplier ratio of two) for reinforcing the temporal features learning ability in each extracted feature maps.

### Step 3. Inverted bottleneck

Based on the proved design recommendation of advanced CNN architectures [Liu et al., 2022, Sandler et al., 2018, Tan and Le, 2019], we modified the network blocks (five blocks based on previous modifications) to the inverted bottleneck structure with an expansion ratio of 4. The final output filters of CNN blocks are 8\*32\*64\*32\*8 (32→64: depthwise convolutions).

### Step 4. Network dilation with fewer activation functions

This step reinforces the network's third part and temporal feature learning ability. Instead of adding sequential NNs like causal padding or TCN block, we adapt different dilations in the third part of the network to avoid further increasing the complexity. We added dilation in both the Conv2D blocks in the third part of the network, 1\*2 and 1\*4, respectively, to gain more global features. Finally, following the suggestions in [Liu et al., 2022], we reduced the activation functions between blocks. Now each part of the network uses a single ELU activation.

All combined steps composite the EEGNeX.

**Closing remarks** We propose a new architecture of the network design after a few more rounds of micro adjustments. Instead of the successful changes mentioned above, some experiences that failed in improvement are as follows:

1. Deeper networks: By simply stacking more convolution layers usually leads to converging difficulty in the training phase with poor performance. Compared with image data, EEG datasets are smaller size-wise. A deep network would earlier confront the overfitting issue.
2. Fewer normalization layers: The modern CNN-based structures in the computer vision domain achieve some improvements by removing some normalization layers. The experience is not applicable in our domain; the reason might lie in the shallow network design.
3. Reordering different parts/layers: We also tried various combinations of parts' orders based on the structure of EEGNet. No improvements were found.
4. Attention block: We implemented a common attention structure: convolutional block attention module (CBAM) [Woo et al., 2018] between parts for channel and spatial attention. No improvements were found.

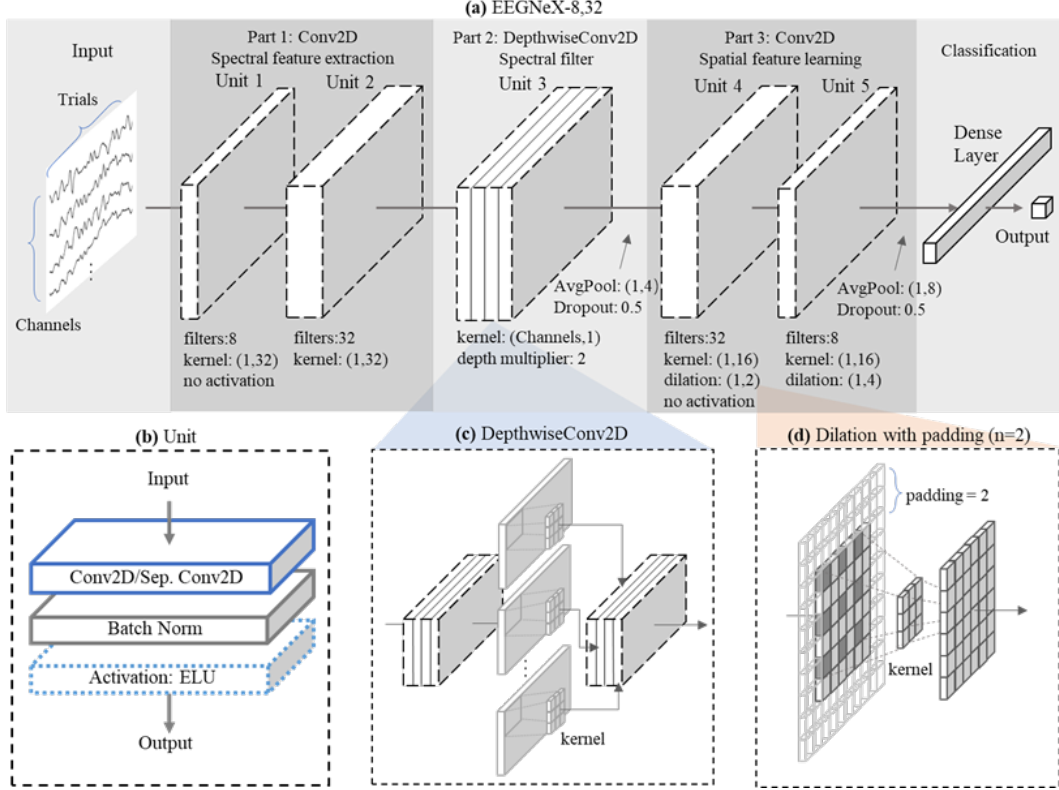
Ultimately, we present a pure convolution-based network – EEGNeX-8,32 that adapts to modern design experience. Accuracies on four datasets achieving a significant improvement compared with EEGNet-8,2. The fixed structure of EEGNeX with full parameter description is presented in Figure 3 and Table 3.

## 4 Performance evaluation

### 4.1 BCI Competition IV Dataset 2a

To validate the efficacy of EEGNeX, we first test its performance with similar advanced methods mentioned in section 2.1 with their shared evaluation dataset: BCI Competition IV dataset 2a (SMR). Three existing methods were selected for performance evaluation: EEG-Inception, EEG-TCNet, and EEG-ITNet. We evaluated within-subject by using the same data processing implementation, resampling rate (125Hz), training strategy with the result described in [Salami et al., 2022]. Three EOG channels available in the dataset were excluded from our analysis.

Table 4 illustrate the comparison result with the test of significance. EEGNeX shows accuracy advance with statistical significance over EEGNet, EEG-Inception, and EEG-TCNet.



#### 4.2 Mother of All BCI Benchmarks

To exhaustively examine the efficacy of EEGNeX in a broader context, 11 open access, multi-classes MI datasets in MOABB [Jayaram and Barachant, 2018] were applied. We benchmark EEGNeX and EEGNet on MOABB by comparing them to three other built-in common non-NN algorithm pipelines in BCIs. These algorithms are:

- CSP + LDA: where trial covariances estimated via maximum-likelihood with unregularized common spatial patterns (CSP). Features were log variance of the filters belonging to the six most diverging eigenvalues and then classified with linear discriminant analysis (LDA).
- TS + optSVM: where trial covariances estimated via oracle approximating shrinkage estimator (OAS) then projected into the Riemannian tangent space to obtain features and classified with a linear SVM with identical grid search.
- AM + optSVM: where features are the log-variance in each channel and then classified with a linear SVM with grid search.

The evaluation was chosen to be within-subject, as that minimizes the effect of non-stationarity. It is worth mentioning that some dataset collections in MOABB own small sample sets of data within-session, which increases the training difficulties of NN algorithms. The accuracy metric scores in 5-fold cross-validation to validate the general feature extraction & representation performance. Figure 4 presents the meta-analysis of the comparison between EEGNeX, EEGNet, and TS+optSVM, which is the state-of-the-art algorithm pipeline on MOABB. Across diverse datasets, the result validates the performance novelty of EEGNeX: it competes favorably with EEGNet methods ( $p < 0.001$ , Wilcoxon tests) and outperforms TS+optSVM ( $p < 0.05$ ).

Block	Layer	# filters	size	# params	Output	Options
1	Input				(C, T)	
	Reshape				(1, C, T)	
	Conv2D	$F_1$	(1, 32)	$32 * F_1$	$(F_1, C, T)$	use_bias = False, padding='same'
2	BatchNorm			$2*T$	$(F_1, C, T)$	
	Conv2D	$F_1 * 4$	(1, 32)	$32 * F_1 * 16$	$(F_1 * 4, C, T)$	use_bias = False, padding='same'
	BatchNorm			$2*T$	$(F_1 * 4, C, T)$	
3	Activation				$(F_1 * 4, C, T)$	ELU
	DepthwiseConv2D	$F_1 * 4 * D$	(C, 1)	$2*T$	$(F_1 * 8, 1, T)$	depth_multiplier= $D$ , use_bias = False, depthwise_constraint=max_norm(1.)
	BatchNorm			$2*T$	$(F_1 * 8, 1, T)$	
	Activation				$(F_1 * 8, 1, T)$	ELU
	AvgPool2D		(1, 4)		$(F_1 * 8, 1, T/4)$	
4	Dropout				$(F_1 * 8, 1, T/4)$	rate = 0.5
	Conv2D	$F_1 * 4 * D$	(1, 16)	$16 * F_1 * 128/4$	$(F_1 * 8, 1, T/4)$	use_bias = False, padding='same', dilation_rate=(1, 2)
	BatchNorm			$2*T/4$	$(F_1 * 8, 1, T/4)$	
	Activation				$(F_1, 1, T/4)$	use_bias = False, padding='same', dilation_rate=(1, 4)
5	Conv2D	$F_1$	(1, 16)	$16 * F_1 * 16/4$	$(F_1, 1, T/4)$	use_bias = False, padding='same', dilation_rate=(1, 4)
	BatchNorm			$2*T/4$	$(F_1, 1, T/4)$	
	Activation				$(F_1, 1, T/4)$	ELU
	AvgPool2D		(1, 8)		$(F_1, 1, T/32)$	
	Dropout				$(F_1, 1, T/32)$	rate = 0.5
Classifier	Flatten			$F_1 * T/32$	$(F_1 * T/32)$	
	Dense				N	kernel_constraint=max_norm(0.25)
	Activation				N	softmax

Table 3: EEGNeX-8,32 architecture, where  $C$ = number of channels,  $T$ = number of timesteps,  $F_1$  = number of temporal filters (8),  $D$ = depth multiplier in DepthwiseConv2D (2), and  $N$ = number of classes, respectively.

	EEG-Inception [Riyad et al., 2020]	EEGNet-8,2 [Lawhern et al., 2018]	EEG-TCNet [Ingolfsson et al., 2020]	EEG-ITNet [Salami et al., 2022]	EEGNeX-8,32
<b>S1</b>	77.43	81.94	82.29	84.38	<b>86.25</b>
<b>S2</b>	54.51	56.94	<b>64.24</b>	62.85	60.71
<b>S3</b>	82.99	90.62	88.89	89.93	<b>93.38</b>
<b>S4</b>	<b>72.22</b>	67.01	60.76	69.10	70.27
<b>S5</b>	73.26	72.57	72.92	<b>74.31</b>	67.14
<b>S6</b>	64.24	58.68	62.50	57.64	<b>70.63</b>
<b>S7</b>	82.64	76.04	83.33	88.54	<b>88.84</b>
<b>S8</b>	77.78	81.25	79.51	83.68	<b>85.89</b>
<b>S9</b>	76.36	78.12	76.39	80.21	<b>86.16</b>
<b>Average</b>	73.50	73.69	74.54	76.74	<b>78.81</b>
<b>Std.</b>	9.11	11.12	10.09	11.48	11.60
<b>p-value</b>	<b>0.011*</b>	<b>0.011*</b>	<b>0.015*</b>	0.146	-

Table 4: Performance results of advanced algorithms for within-subject evaluation of BCI Competition IV Dataset 2a in terms of classification accuracy. Star \* corresponds to significant at level of 0.05.

Figure 5 summarizes the ranking of algorithms in performance with statistics generated across all 11 datasets in MOABB. The result underlines that EEGNeX generalized well across all datasets and outperformed other algorithm pipelines. We concluded that the general structure modifications to EEGNeX (increased layer depth, inverted bottleneck, dilation) and micro adjustment are universally valid for accuracy improvement in EEG-based BCI classification tasks.

In the end, we open-sourced code in Keras for easy, out-of-box reproduction to use in different research sources (<https://github.com/chenxiachan/EEGNeX>). All models are coded in the same implementation format with input in the shape of  $(trials * channels * timesteps)$ , and one-hot-encoded output. We designed an experiment to run all models on the dataset for ten rounds with random seeds to record their accuracy performances for statistical tests.

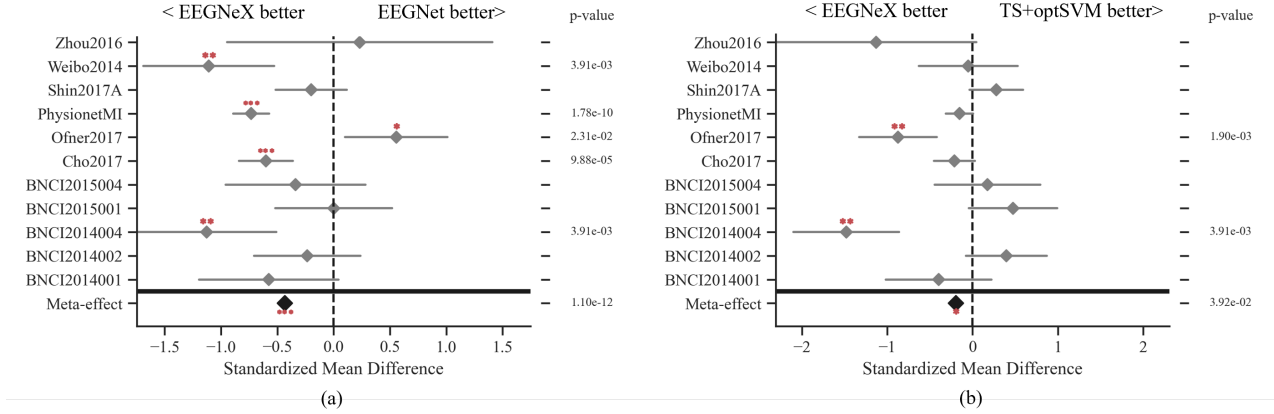


Figure 4: Meta-analysis comparing EEGNeX against EEGNet (a) and the state-of-the-art algorithm pipeline on MOABB: TS-optSVM (b). The result is evaluated by within-recoding-session accuracy. The effect sizes shown are standardized mean differences, with p-values corresponding to the one-tailed Wilcoxon signed-rank test for the hypothesis given at the top of the plot and 95% interval denoted by the grey bar. Stars correspond to \*\*\* =  $p < 0.001$ , \*\* =  $p < 0.01$ , \* =  $p < 0.05$ . The meta-effect is shown at the bottom of the plot. The overall trend shows that EEGNeX is on average better than EEGNet and TS-optSVM.

Algorithm comparison					
	AM+optSVM				
csp+lda	0.58 p=5e-10				
EEGNet-8,2	0.68 p=2e-08	0.22 p=4e-02			
TS+optSVM	1.10 p=1e-25	0.48 p=3e-11			
EEGNeX-8,32	0.93 p=2e-18	0.50 p=2e-08	0.43 p=9e-13	0.19 p=4e-02	
	AM+optSVM	csp+lda	EEGNet-8,2	TS+optSVM	EEGNeX-8,32

Figure 5: Ranking of algorithms in performance across all datasets. As all p-values are single-sided for clarity. The values correspond to the standardized mean difference of the algorithm in the y-axis minus that in the x-axis and the associated p-value. The comparison shows the meta-effect in case that the method on the vertical axis significantly outperforms the method on the horizontal axis, according to the one-tailed Wilcoxon signed-rank test.

## 5 Discussion

The thought in our brain, has been using mainly language to interact with the world for a long period. Just as Ludwig Josef Johann Wittgenstein [Wittgenstein, 2013] described:

*“The limits of my language mean the limits of my world.”*

Now, the BCI study creates a direct communication pathway for decoding brain’s activities, revealing a huge potential for establishing new patterns for human-computer interaction (HCI). By the generalization power of NNs, we foresee that the effort invested in interpreting brain activities would benefit a broad branch of domains, from information & communications technology to medical, from social science to design, and even revolutionize how we perceive and understand reality. Take the design domain as an example; new BCI patterns would efficiently assist designers in expressing and interacting with the design work: their personal preferences, less expressible feelings, and subconscious perceptions can be captured, represented, and transferred more seamlessly via the brain’s electrical signals without

explicitly formalizing in languages or actions. Starting with the EEG classification, this study aims to minimize the gap between the BCI domain study and efficient NNs implementation. It offers a testbed for different network architectures comparison to encourage more interdisciplinary research participation. From this perspective, the construction of our open-source testbed remains primitive.

Based on the analysis result within the scope of this study, it is natural to conclude: the design of RNN-based and time-domain architecture of NN models is practically less efficient in EEG information representation than CNNs. In other words, NN techniques designed for local attention in sequential information decoding are generally not as efficient as global information extraction by moving receptive fields. The depthwise layer with enhanced performance further corroborates this viewpoint.

The limitation of this study is: The intention of designing this benchmark is to include diverse NN architectures in the research of reliable EEG signal decoding paths. We referred to ConvNeXt to find the path shortcut for improved efficiency by the convolution inductive bias. Although the original ConvNeXt claims the performance advance in the CV domain, image classification tasks than Transformer, the contribution of different mechanisms in four pillars mentioned in Figure 1 is still worth investigating in the BCI domain. Besides the performance advance of CNN-based methods, we noticed from the benchmark result that the hybrid-model approach owns accuracy improvement over single architecture from its composition, which reveals a deeper EEG representation question. The reason is that the BCI signal data, in essential, combines characteristics from both the sequential format of NLP and the multi-channels from image data in CV. We observed several research attempts to adopt the BCI data in both branches [Craik et al., 2019b, Hosseini et al., 2020]. In this context, the hybrid-model approach by deeply combining CNN and RNN architecture, the decent design of acquiring long-range global features in sequence by self-attention in Transformer, dimension reduction by encoder-decoder, and more NN techniques own potential for further improvement.

When aiming for a generalization evaluation, it might be ideal for future research to test the decoding performance of EEGNeX using time series data from other imaging modalities, such as magnetoencephalography (MEG) and functional near-infrared spectroscopy (fNIRS). For the utility, it is worth mentioning that although the model is developed based on the EEG task challenges. The benchmark methods and the improvement conducted in the EEGNeX architecture rarely encode know-how feature engineering in the EEG domain specifically. Broader test scenarios within the scope of biological signal decoding in BCI topics could also benefit from this study.

## 6 Conclusion

In this study, we conducted large-scale NNs' efficacy experiments to test their performance in EEG-based BCI classification tasks. The accuracy and EEG information representation ability of neural networks with different structures were sorted out by comparing the results. Four pillars to design an efficient NN model for EEG classification are proposed based on the result.

Built on the result analysis, we proposed a novel model: EEGNeX, a pure convolution-based network. Improvements are mainly adopted from neural network representation studies. We tested the EEGNeX in diverse EEG classification tasks to validate its universal efficacy. Since the performance improvement is less benefited by case-specific designs, EEGNeX owns the flexibility to combine with knowledge-based, domain feature engineering for variate scenarios adaptations. We hope that the results reported in this study and the benchmark will alleviate the difficulties of model implementation in various BCI studies and accelerate the path toward the representation study in this domain.

## 7 Appendix

### 7.1 Benchmark model structures

Single_GRU	Single_LSTM			
Layer	Layer	# units	size	Options
Input	Input		/	
GRU	LSTM	100	/	return_sequences=True, kernel_regularizer=l2(0.0001)
GRU	LSTM	100	/	return_sequences=True, kernel_regularizer=l2(0.0001)
GRU	LSTM	100	/	kernel_regularizer=l2(0.0001)
Dropout	Dropout		/	rate = 0.5
Dense	Dense	100	/	activation='elu'
Dense	Dense		/	activation='softmax'

Table 5: The architecture of GRU and LSTM; They both share the same general structure but with different RNN layer.

			1D_CNN	1D_CNN_Dilated	1D_CNN_Causal	1D_CNN_CausalDilated	
Layer	# filters	size	Options	Options	Options	Options	Options
Input							
Conv1D	64	3	/	/	padding='causal'	padding='causal'	
BatchNorm							
Activation			elu				
Conv1D	64	3	/	dilation_rate=2	padding='causal'	padding='causal', dilation_rate=2	
BatchNorm							
Activation			elu				
Conv1D	64	3	/	/	padding='causal'	padding='causal'	
BatchNorm							
Activation			elu				
Dropout			rate = 0.5				
MaxPooling1D			pool_size=2				
Flatten							
Dense	100		activation='elu'				
Dense			activation='softmax'				

Table 6: The architecture of 1D CNN models; They share the same general structure but with different layer parameter options.

			2D_CNN	2D_CNN_Dilated
Layer	# filters	size	Options	Options
Input				
Conv2D	64	(1, 3)		
BatchNorm				
Activation			elu	
Conv2D	64	(1, 3)	/	dilation_rate=2
BatchNorm				
Activation			elu	
Conv2D	64	(1, 3)		
BatchNorm				
Activation			elu	
Dropout			rate = 0.5	
AvgPooling2D			pool_size=2, padding='same'	
Flatten				
Dense	100		activation='elu'	
Dense			activation='softmax'	

Table 7: The architecture of 2D CNN models; They share the same general structure but with different layer parameter setting options.

2D_CNN_Depthwise	2D_CNN_Separable			
Layer	Layer	# filters	size	Options
Input	Input			
DepthwiseConv2D	SeparableConv2D	64	(1, 3)	
BatchNorm	BatchNorm			
Activation	Activation			elu
SeparableConv2D	SeparableConv2D	64	(1, 3)	
BatchNorm	BatchNorm			
Activation	Activation			elu
SeparableConv2D	SeparableConv2D	64	(1, 3)	
BatchNorm	BatchNorm			
Activation	Activation			elu
Dropout	Dropout			rate = 0.5
AvgPooling2D	AvgPooling2D			pool_size=2, padding='same'
Flatten	Flatten			
Dense	Dense	100		activation='elu'
Dense	Dense			activation='softmax'

Table 8: The architecture of Depthwise and Separable 2D CNN.

Single_ConvLSTM2D			
Layer	# filters	size	Options
Input			
ConvLSTM2D	64	(1,3)	kernel_regularizer=l2(0.0001)
BatchNorm			
Activation			elu
Dropout			
Flatten			
Dense	100		activation='elu'
Dense			activation='softmax'

Table 9: The architecture of single 2D CNN with LSTM layer.

CNN_GRU	CNN_LSTM			
Layer	Layer	# filters	size	Options
Input	Input			TimeDistributed
Conv1D	Conv1D	64	3	TimeDistributed
BatchNorm	BatchNorm			
Activation	Activation			elu
Conv1D	Conv1D	64	3	TimeDistributed
BatchNorm	BatchNorm			
Activation	Activation			elu
Conv1D	Conv1D	64	3	TimeDistributed
BatchNorm	BatchNorm			
Activation	Activation			elu
Dropout	Dropout			TimeDistributed, rate = 0.5
MaxPooling1D	MaxPooling1D			TimeDistributed, pool_size=2
Flatten	Flatten			TimeDistributed
GRU	LSTM	480		kernel_regularizer=l2(0.0001)
Dropout	Dropout			rate = 0.5
Dense	Dense	100		activation='elu'
Dense	Dense			activation='softmax'

Table 10: The architecture of hybrid-models; They both share the same general structure but with different RNN layer.

## References

Jonathan R. Wolpaw, Niels Birbaumer, William J. Heetderks, Dennis J. McFarland, P. Hunter Peckham, Gerwin Schalk, Emanuel Donchin, Louis A. Quatrano, Charles J. Robinson, Theresa M. Vaughan, et al. Brain-computer interface technology: a review of the first international meeting. *IEEE transactions on rehabilitation engineering*, 8(2):164–173, 2000.

Jürgen Schmidhuber. Deep learning in neural networks: An overview. *Neural networks*, 61:85–117, 2015.

Uri Hasson, Samuel A. Nastase, and Ariel Goldstein. Direct fit to nature: an evolutionary perspective on biological and artificial neural networks. *Neuron*, 105(3):416–434, 2020.

Ernst Niedermeyer and F. LopesH Da Silva. *Electroencephalography: basic principles, clinical applications, and related fields*. Lippincott Williams & Wilkins, 2005.

Sepp Hochreiter and Jürgen Schmidhuber. Long short-term memory. *Neural computation*, 9(8):1735–1780, 1997.

Junyoung Chung, Caglar Gulcehre, KyungHyun Cho, and Yoshua Bengio. Empirical evaluation of gated recurrent neural networks on sequence modeling. *arXiv preprint arXiv:1412.3555*, 2014.

Giulio Ruffini, David Ibañez, Marta Castellano, Stephen Dunne, and Aureli Soria-Frisch. Eeg-driven rnn classification for prognosis of neurodegeneration in at-risk patients. In *International Conference on Artificial Neural Networks*, pages 306–313, 2016.

Alexander Craik, Yongtian He, and Jose L. Contreras-Vidal. Deep learning for electroencephalogram (eeg) classification tasks: a review. *Journal of neural engineering*, 16(3):031001, 2019a.

Laith Alzubaidi, Jinglan Zhang, Amjad J Humaidi, Ayad Al-Dujaili, Ye Duan, Omran Al-Shamma, José Santamaría, Mohammed A Fadhel, Muthana Al-Amidie, and Laith Farhan. Review of deep learning: Concepts, cnn architectures, challenges, applications, future directions. *Journal of big Data*, 8(1):1–74, 2021.

Hamdi Altaheri, Ghulam Muhammad, Mansour Alsulaiman, Syed Umar Amin, Ghadir Ali Altuwaijri, Wadood Abdul, Mohamed A. Bencherif, and Mohammed Faisal. Deep learning techniques for classification of electroencephalogram (eeg) motor imagery (mi) signals: a review. *Neural Computing and Applications*, pages 1–42, 2021.

Vernon J. Lawhern, Amelia J. Solon, Nicholas R. Waytowich, Stephen M. Gordon, Chou P. Hung, and Brent J. Lance. Eegnet: a compact convolutional neural network for eeg-based brain–computer interfaces. *Journal of neural engineering*, 15(5):056013, 2018.

Xin Deng, Boxian Zhang, Nian Yu, Ke Liu, and Kaiwei Sun. Advanced tsgl-eegnet for motor imagery eeg-based brain-computer interfaces. *IEEE Access*, 9:25118–25130, 2021.

Wenkai Huang, Yihao Xue, Lingkai Hu, and Hantang Liuli. S-eegnet: Electroencephalogram signal classification based on a separable convolution neural network with bilinear interpolation. *IEEE Access*, 8:131636–131646, 2020.

Vinay Jayaram and Alexandre Barachant. Moabb: trustworthy algorithm benchmarking for bcis. *Journal of neural engineering*, 15(6):066011, 2018.

Hubert Cecotti and Axel Graser. Convolutional neural networks for p300 detection with application to brain-computer interfaces. *IEEE transactions on pattern analysis and machine intelligence*, 33(3):433–445, 2010.

Robin Tibor Schirrmeister, Jost Tobias Springenberg, Lukas Dominique Josef Fiederer, Martin Glasstetter, Katharina Eggensperger, Michael Tangermann, Frank Hutter, Wolfram Burgard, and Tonio Ball. Deep learning with convolutional neural networks for eeg decoding and visualization. *Human brain mapping*, 38(11):5391–5420, 2017.

Zheng Yang Chin, Kai Keng Ang, Chuanchu Wang, Cuntai Guan, and Haihong Zhang. Multi-class filter bank common spatial pattern for four-class motor imagery bci. In *2009 Annual International Conference of the IEEE Engineering in Medicine and Biology Society*, pages 571–574, 2009.

Mouad Riyad, Mohammed Khalil, and Abdellah Adib. Incep-eegnet: a convnet for motor imagery decoding. In *International Conference on Image and Signal Processing*, pages 103–111, 2020.

Ravikiran Mane, Effie Chew, Karen Chua, Kai Keng Ang, Neethu Robinson, A. Prasad Vinod, Seong-Whan Lee, and Cuntai Guan. Fbcnet: A multi-view convolutional neural network for brain-computer interface. *arXiv preprint arXiv:2104.01233*, 2021.

Thorir Mar Ingolfsson, Michael Hersche, Xiaying Wang, Nobuaki Kobayashi, Lukas Cavigelli, and Luca Benini. Eeg-tcnet: An accurate temporal convolutional network for embedded motor-imagery brain-machine interfaces. In *2020 IEEE International Conference on Systems, Man, and Cybernetics (SMC)*, pages 2958–2965, 2020.

Shaojie Bai, J. Zico Kolter, and Vladlen Koltun. An empirical evaluation of generic convolutional and recurrent networks for sequence modeling. *arXiv preprint arXiv:1803.01271*, 2018.

Abbas Salami, Javier Andreu-Perez, and Helge Gillmeister. Eeg-itnet: An explainable inception temporal convolutional network for motor imagery classification. *IEEE Access*, 10:36672–36685, 2022.

Salma Alhagry, Aly Aly Fahmy, and Reda A. El-Khoribi. Emotion recognition based on eeg using lstm recurrent neural network. *Emotion*, 8(10):355–358, 2017.

Ping Wang, Aimin Jiang, Xiaofeng Liu, Jing Shang, and Li Zhang. Lstm-based eeg classification in motor imagery tasks. *IEEE transactions on neural systems and rehabilitation engineering*, 26(11):2086–2095, 2018.

Ashish Vaswani, Noam Shazeer, Niki Parmar, Jakob Uszkoreit, Llion Jones, Aidan N. Gomez, Łukasz Kaiser, and Illia Polosukhin. Attention is all you need. *Advances in neural information processing systems*, 30, 2017.

J. X. Chen, D. M. Jiang, and Y. N. Zhang. A hierarchical bidirectional gru model with attention for eeg-based emotion classification. *IEEE Access*, 7:118530–118540, 2019.

Theerawit Wilaiprasitporn, Apiwat Ditthapron, Karis Matchaparn, Tanaboon Tongbuasirilai, Nannapas Banluesombatkul, and Ekapol Chuangsawanich. Affective eeg-based person identification using the deep learning approach. *IEEE Transactions on Cognitive and Developmental Systems*, 12(3):486–496, 2019.

Jacob Devlin, Ming-Wei Chang, Kenton Lee, and Kristina Toutanova. Bert: Pre-training of deep bidirectional transformers for language understanding. *arXiv preprint arXiv:1810.04805*, 2018.

Alexey Dosovitskiy, Lucas Beyer, Alexander Kolesnikov, Dirk Weissenborn, Xiaohua Zhai, Thomas Unterthiner, Mostafa Dehghani, Matthias Minderer, Georg Heigold, Sylvain Gelly, et al. An image is worth 16x16 words: Transformers for image recognition at scale. *arXiv preprint arXiv:2010.11929*, 2020.

Karen Simonyan and Andrew Zisserman. Very deep convolutional networks for large-scale image recognition. *arXiv preprint arXiv:1409.1556*, 2014.

Kaiming He, Xiangyu Zhang, Shaoqing Ren, and Jian Sun. Deep residual learning for image recognition. In *Proceedings of the IEEE conference on computer vision and pattern recognition*, pages 770–778, 2016.

Mingxing Tan and Quoc Le. Efficientnet: Rethinking model scaling for convolutional neural networks. In *International conference on machine learning*, pages 6105–6114, 2019.

Zhuang Liu, Hanzi Mao, Chao-Yuan Wu, Christoph Feichtenhofer, Trevor Darrell, and Saining Xie. A convnet for the 2020s. *arXiv preprint arXiv:2201.03545*, 2022.

Martín Abadi, Ashish Agarwal, Paul Barham, Eugene Brevdo, Zhifeng Chen, Craig Citro, Greg S Corrado, Andy Davis, Jeffrey Dean, Matthieu Devin, et al. Tensorflow: Large-scale machine learning on heterogeneous distributed systems. *arXiv preprint arXiv:1603.04467*, 2016.

François Chollet. Xception: Deep learning with depthwise separable convolutions. In *Proceedings of the IEEE conference on computer vision and pattern recognition*, pages 1251–1258, 2017.

Aäron van den Oord, Sander Dieleman, Heiga Zen, Karen Simonyan, Oriol Vinyals, Alex Graves, Nal Kalchbrenner, Andrew W. Senior, and Koray Kavukcuoglu. Wavenet: A generative model for raw audio. *SSW*, 125:2, 2016.

Fisher Yu and Vladlen Koltun. Multi-scale context aggregation by dilated convolutions. *arXiv preprint arXiv:1511.07122*, 2015.

Mohammad-Parsa Hosseini, Amin Hosseini, and Kiarash Ahi. A review on machine learning for eeg signal processing in bioengineering. *IEEE reviews in biomedical engineering*, 14:204–218, 2020.

Sergey Ioffe and Christian Szegedy. Batch normalization: Accelerating deep network training by reducing internal covariate shift. In *International conference on machine learning*, pages 448–456, 2015.

Anish Shah, Eashan Kadam, Hena Shah, Sameer Shinde, and Sandip Shingade. Deep residual networks with exponential linear unit. In *Proceedings of the Third International Symposium on Computer Vision and the Internet*, pages 59–65, 2016.

D. Vivancos. Mindbigdata the 'mnist' of brain digits, 2020. URL <http://www.mindbigdata.com/opendb/>.

Min-Ho Lee, O-Yeon Kwon, Yong-Jeong Kim, Hong-Kyung Kim, Young-Eun Lee, John Williamson, Siamac Fazli, and Seong-Whan Lee. Eeg dataset and openbmi toolbox for three bci paradigms: an investigation into bci illiteracy. *GigaScience*, 8(5):giz002, 2019.

Michael Tangermann, Klaus-Robert Müller, Ad Aertsen, Niels Birbaumer, Christoph Braun, Clemens Brunner, Robert Leeb, Carsten Mehring, Kai J. Müller, Gernot Mueller-Putz, et al. Review of the bci competition iv. *Frontiers in neuroscience*, page 55, 2012.

Perrin Margaux, Maby Emmanuel, Daligault Sébastien, Bertrand Olivier, and Mattout Jérémie. Objective and subjective evaluation of online error correction during p300-based spelling. *Advances in Human-Computer Interaction*, 2012, 2012.

Andrew G. Howard, Menglong Zhu, Bo Chen, Dmitry Kalenichenko, Weijun Wang, Tobias Weyand, Marco Andreetto, and Hartwig Adam. Mobilenets: Efficient convolutional neural networks for mobile vision applications. *arXiv preprint arXiv:1704.04861*, 2017.

Mark Sandler, Andrew Howard, Menglong Zhu, Andrey Zhmoginov, and Liang-Chieh Chen. Mobilenetv2: Inverted residuals and linear bottlenecks. In *Proceedings of the IEEE conference on computer vision and pattern recognition*, pages 4510–4520, 2018.

Sanghyun Woo, Jongchan Park, Joon-Young Lee, and In So Kweon. Cbam: Convolutional block attention module. In *Proceedings of the European conference on computer vision (ECCV)*, pages 3–19, 2018.

Ludwig Wittgenstein. *Tractatus logico-philosophicus*. Routledge, 2013.

Alexander Craik, Yongtian He, and Jose L. Contreras-Vidal. Deep learning for electroencephalogram (eeg) classification tasks: a review. *Journal of neural engineering*, 16(3):031001, 2019b.